Monitoring of Glass Transition at a Polymer Surface by Localized Surface Plasmon Resonance

Ratan K. Putla and A. Kaan Kalkan
Oklahoma State University, Stillwater, OK, USA, ratan@okstate.edu, kaan.kalkan@okstate.edu

ABSTRACT

The present work investigates glass transition at the surface of a polymer by means of localized surface plasmon resonance (LSPR), associated with gold nanoparticles (Au NPs). Au NPs at an average size of 8 nm, were vacuum deposited on poly isobutyl methacrylate (PiBMA) films. Subsequently, time series LSPR spectra of NPs on PiBMA were acquired in a temperature controlled optical cell. The penetration of Au NPs into polymer induces a shift in LSPR spectra due to altering dielectric environment encompassing the NPs. The effective dielectric constant surrounding the NPs was deduced from the LSPR optical extinction peak. Then, depth and velocity of penetration were derived from the effective dielectric constant. The onset of NP penetration was found to be at between 40 and 45 ºC, which is below the reported glass transition of PiBMA by 10 to 15 ºC. A steady penetration velocity was observed until complete embedding that was found to be temperature activated at 0.65 eV.

Keywords: glass transition, plasmon, nanoparticles, poly isobutyl methacrylate, surface

1 INTRODUCTION

Investigations on polymer surfaces by various groups have revealed that the glass transition temperature at the surface, T_{gs}, is not equal to that in the bulk, T_{gb}. In 2003, Teichroeb and Forrest monitored embedding of Au NPs into polystyrene surface by atomic force microscopy and suggested the existence of a more mobile surface region about 3-4 nm thick, indicative of $T_{gs} < T_{gb}$ [1]. However, in 2005 Hutcheson and McKenna argued against this proposition of Teichroeb and Forrest using a visco-elastic contact mechanics model that the embedding of Au NPs was due to the indentation created by the large surface interaction between polystyrene and Au and not due to the existence of a so called "liquid like layer" [2]. After the controversy raised by these studies, it is understood that a better understanding of T_{gs} for polymers has yet to be attained. Accordingly, there are several open questions to be addressed: is T_{gs} equal /above/ below T_{gb}? Is the polymer surface viscous/visco-elastic at a temperature equal or higher than T_{gs} but lower than melting temperature.

The interaction of light with the conduction electrons in NPs results in collective oscillations of the electrons which are known as localized surface plasmons (LSPs). LSPs can be resonantly excited by light at a certain frequency known as the plasmon frequency and the resonance condition is called localized surface plasmon resonance (LSPR) [3]. Plasmon frequency will shift with the variation in dielectric constant of the surrounding medium. This spectral shift forms the basis of detection in LSPR sensors. LSPR sensing can monitor the dielectric variations around the NP within a few nm of the NP surface. The photons coupled with the LSP localize to close vicinity of the NP creating enhanced electromagnetic near fields. As a result, LSPR is susceptible to the close vicinity of the NP, while the variation in LSPR can be reported to the far field in terms of scattering or absorption.

In this work, we exploit these unique attributes of LSPR to study the glass transition phenomenon at the surface of a polymer. When the surface of a polymer is above the glass transition temperature, the nanoparticles dispersed on this surface undergo embedding, which is driven by the minimization of free energy. The impregnation of NPs into the polymer is expected to cause spectral shift in LSPR of NPs due to the changing dielectric environment surrounding NPs. Because plasmon resonance fields are localized within a few nm from the NP surfaces, the signal will be selectively captured from the polymer region, which is within few nm of polymer/air interface. On the other hand, if an objective lens is employed to probe the polymer surface, the spatial resolution is diffraction limited to the wavelength of light. Hence, by our approach, diffraction limit of light can be overcome as the impregnation of NP into the polymer can be monitored to a spatial resolution down to a nanometer.

2 THEORETICAL MODEL

In 1908, Gustav Mie solved the Maxwell's equations and obtained the extinction cross section of a solid sphere, σ_{ext}, in an electromagnetic field of angular frequency ω given by:

$$\sigma_{ext}(\omega) = 9\frac{\omega}{c}\varepsilon_m^{3/2}V\left(\frac{\varepsilon_2(\omega)}{[[\varepsilon_1(\omega)+2\varepsilon_m]^2+[\varepsilon_2(\omega)]^2]}\right) \quad (1)$$

where, $[\varepsilon_1(\omega) + i\varepsilon_2(\omega)]$ and ε_m are the dielectric functions for the sphere and the surrounding medium, respectively [1]. V is the sphere's volume, and c is the velocity of light. Clearly, σ_{ext} has a resonance for $\varepsilon_1(\omega) + 2\varepsilon_m = 0$, or $\varepsilon_1(\omega) = -2\varepsilon_m$, $at\ \omega = \omega_{lsp}$. From the free electron theory and accounting for the deviations from the free electron behavior (i.e., interactions with atomic cores, intra and inter-band transitions), ε_d :

$$\varepsilon_1(\omega) = 1 - \left(\frac{\lambda}{\lambda_p}\right)^2 + \varepsilon_d \quad (2)$$

where, λ_p is the bulk plasmon wavelength. Hence,

$$\varepsilon_m = \frac{1}{2}\left(\frac{\lambda_{isp}^2}{\lambda_p^2} - \varepsilon_d - 1\right) \quad (3)$$

Moreover, the effective dielectric constant is the sum of the contributions from the near field, ε_n, and the evanescent field, ε_e:

$$\varepsilon_m = \varepsilon_n + \varepsilon_e \quad (4)$$

Considering a sphere of radius R partially sunk in the polymer at a depth of x, the electromagnetic coupling of the NP with its surroundings occurs in a skinny region surrounding the particle. Accordingly, a spherical shell of thickness δ ($\ll R,\ radius\ of\ the\ sphere$) surrounding the NP is considered. Then the average density of molecules, $N(x)$, situated in this volume is given by

$$N(x) = \frac{N_p A(x)\delta}{4\pi R^2 \delta} \quad (5)$$

where $A(x)$ is the surface area of the sphere in contact with the polymer, N_p is the molecular density of the polymer. At full penetration, $N(x = 2R) = N_p$. Furthermore,

$$A(x) = \int_{\theta=0}^{2\pi}\int_{\phi=0}^{\phi(x)} R^2 \sin\phi \, d\phi d\theta = 2\pi R x \quad (6)$$

Also, since $Rcos\,\varphi(x) = R - x$, Equation 5 resumes to

$$N(x) = \frac{1}{2}N_p(x/R) \quad (7)$$

The next step is to relate $\varepsilon_n(x)$ to $N(x)$ as:

$$\varepsilon_n(x) = 1 + \frac{N(x)\alpha}{\varepsilon_0} \quad (8)$$

where, N is the number of dipoles (e.g., mers) per unit volume, α is the molecular polarizability (i.e., for a mer), and ε_0 is the permittivity of the free space. Hence from Equations 7 and 8 we get:

$$\varepsilon_n(x) = 1 + \frac{N_p\alpha}{\varepsilon_0}\left(\frac{x}{2R}\right) \quad (9)$$

Finally, combining Equations (3), (4) and (9)

$$\varepsilon_m(x) = \varepsilon_e + \frac{N_p\alpha}{\varepsilon_0}\left(\frac{x}{2R}\right) \quad (10)$$

$\varepsilon_e = \varepsilon_m(x = 0)$ is obtained prior to embedding, and $\left(\frac{x}{2R}\right)$ during embedding can be derived from the value of ε_m, which is acquired from LSPR.

3 EXPERIMENTAL PROCEDURE

3 wt% PiBMA in acetone was spin coated on the 1" × 1" Corning code 1737 glass substrates at 1500 rpm yielding approximately 200 nm thick films. The films were cured for 20 h at 60 °C on the hot plate, which is higher than the T_{gs} of PiBMA (i.e., 55 °C). Finally, the sample was coated with 0.8 nm thick layer of Au NPs by physical vapor deposition technique. A StellarNet EPP 2000Cs UV-Vis spectrometer (2048 pixel CCD detector, 2400 g/mm grating, 2 nm optical resolution, 200 µm slit size, deuterium + tungsten - halogen light source) was employed for acquisition of optical extinction. The sample was diced to 1" × 0.5" size and immobilized inside an optical cell. From the recorded extinction spectrum the optical extinction of Au NPs was obtained by subtracting the extinction of PiBMA coated glass substrate without Au NPs from the extinction of PiBMA coated glass substrate with Au NPs. For this purpose, a reference (PiBMA coated glass substrate without Au NPs) was employed. The present investigation requires a temperature control system that offers high precision and fast stabilization. Hence, a custom-made temperature control system was built as illustrated in Fig. 1. First, Ar from the gas cylinder flows through a filament-heated glass tube. The tungsten coil wound around the tube is powered by a VARIAC which allows temperature control by varying the power through the heating coil. Subsequently, heated Ar is guided into the optical cell containing the polymer. The sample is thus heated uniformly by means of forced convection heat transfer by Ar flow inside the optical cell. In addition, forced convection provides quick stabilization of the temperature. During the measurement, the temperature showed minimal fluctuations within ± 0.5 °C of the targeted temperature. Finally, Ar flow exits the optical cell through an outlet needle. The flow rate of Ar was 125 cc/s. A K-type thermocouple is inserted into the optical cell for monitoring the sample temperature. The tip of the thermocouple probe is positioned within 1 mm of the sample surface.

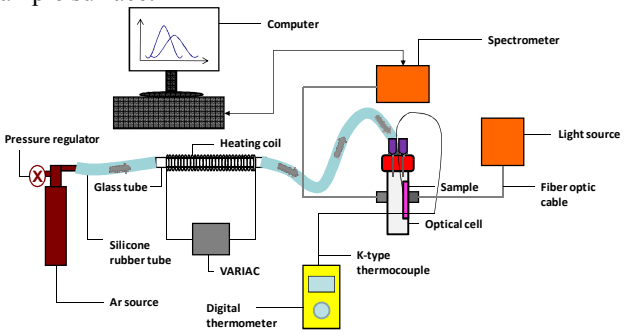

Figure 1: Illustration of the custom-made temperature control system integrated with data acquisition system.

4 RESULTS AND DISCUSSION

The initial investigation involved subjecting the sample to a set of increasing temperatures from 25 to 70 °C with 5

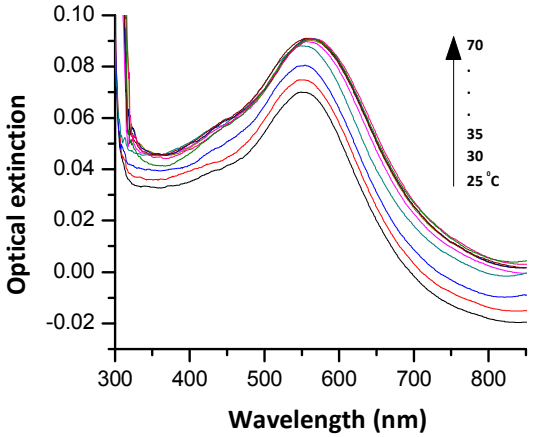

Figure 2: Temperature series spectra of Au NPs on PiBMA.

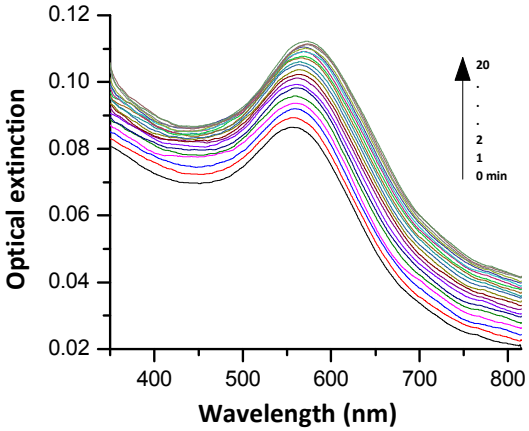

Figure 4: Time series extinction spectra of Au NPs on PiBMA at 55 °C during the first 20 minutes.

°C increments. At each temperature step, the sample was maintained for 10 min before recording the optical extinction of Au NPs. The extinction spectra are shown in Fig. 2 and the corresponding peak wavelength vs. temperature is given in Fig. 3. Since the extinction spectra exhibited a level of noise the data acquired throughout the experiment was smoothened by Savitzky-Golay polynomial regression with the objective of accurate determination of the peak wavelength.

Fig. 3 shows that the optical extinction peak wavelength of Au NPs remains constant until the temperature of the sample reaches 40 °C. However, when the temperature reaches 45 °C, the peak wavelength is found to have red shifted by 4 nm implying a change in ε_m and hence starting of the particle embedding. Thus, the observed peak shift suggests a transition in the polymer surface from rigid to viscous state. Hence, for PiBMA T_{gs} must be between 40 and 45 °C. The viscous state of the polymer surface allows the polymer flow around the NPs and adsorb on the NP surface for minimization of the surface energy. Hence, the problem can be viewed as either embedding of NPs into polymer surface or flow of polymer around NP. Interestingly, the data of Fig. 3 imply an offset of 10 °C or more between the T_{gs} (between 40-45 °C) and Tgb (55 °C). To study the kinetics of Au NP penetration into PiBMA surface, time series LSPR optical extinction spectra of Au NPs were acquired at four different temperatures: 45, 55, 60 and 65 °C. Fig. 4 and 5 show time series extinction spectra of Au NPs on PiBMA surface at 55 °C and corresponding peak shifts in the extinction wavelength of NPs respectively. It is observed that the peak shift of extinction wavelength is almost linear with time before saturation (complete embedding of NPs into the polymer). Fig. 6 compares the kinetics of extinction peak wavelength while Fig. 7 compares the normalized penetration depth (X=x/2R) of Au NPs for 4 different temperatures: 45, 55, 60 and 65 °C. A systematic increase of embedding rate of Au NPs with temperature is inferred. Increased embedding rate is due to the reduced viscosity of the polymer. Neglecting the inertial forces, the surface energy induced force on a NP must be balanced by the

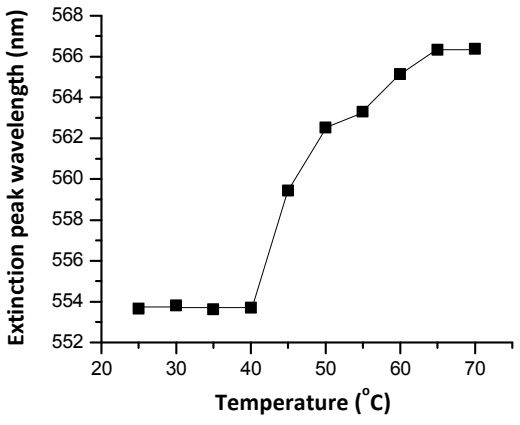

Figure 3: Optical extinction peak (wavelength) versus temperature of Au NPs on PiBMA.

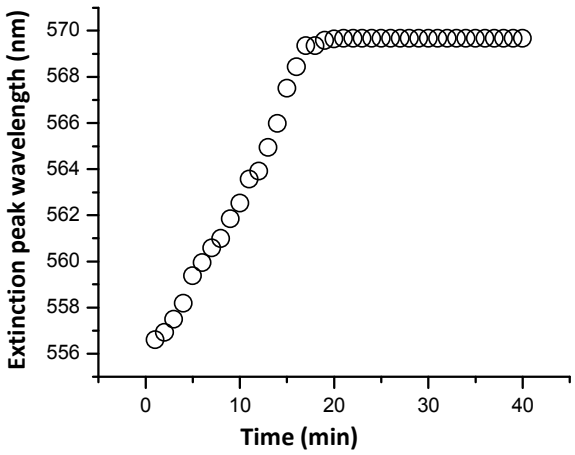

Figure 5: Kinetics of LSPR peak wavelength for Au NPs on PiBMA at 55 °C.

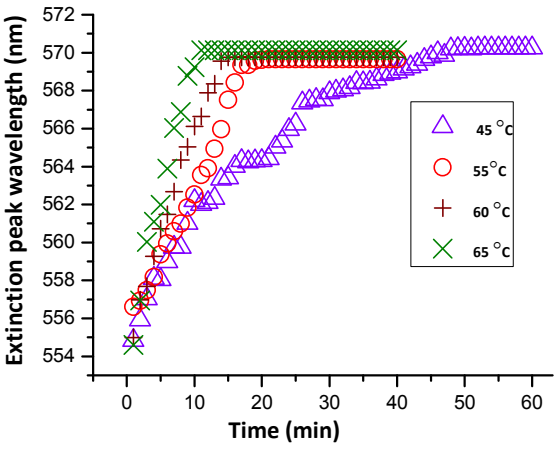

Figure 6. Kinetics of LSPR peak wavelength for Au NPs on PiBMA at 45, 55, 60 and 65 °C.

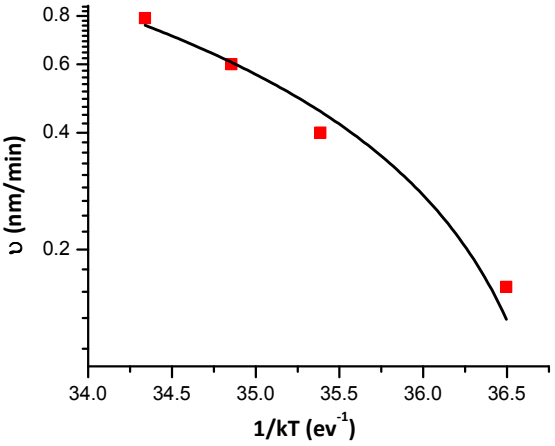

Figure 8: Rate of penetration of Au NPs into PiBMA against $1/kT$.

viscous force. Because, the viscous force is a product of viscosity and shear rate, the increasing penetration rate with temperature suggests decreasing viscosity with temperature. The extinction peak saturates to the same wavelength of 570 nm irrespective of temperature. This result indicates the Au NPs embed into the polymer at the same volume fraction independent of temperature and most likely complete embedding.

Fig. 8 shows the semi- logarithmic relation between the penetration rate vs. 1/kT where, k is the Boltzmann's constant and T is temperature in Kelvin. From the plot the rate of penetration $1/kT$ reveals a Boltzman factor $= e^{(-E_a/kT)}$ above 45 °C for which the activation energy, E_a, is found to be 0.65 eV.

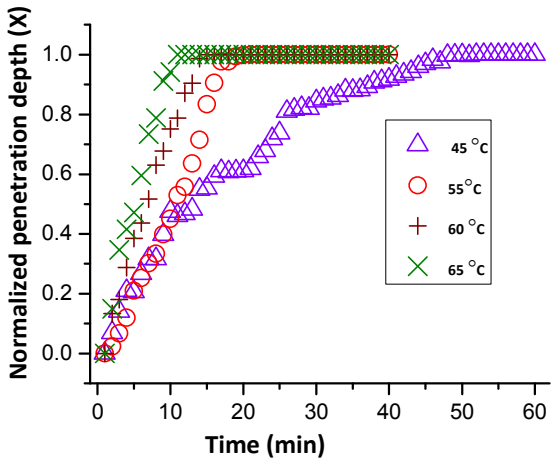

Figure 7: Kinetics of normalized penetration depth for Au NPs on PiBMA at 45, 55, 60 and 65 °C.

At the molecular scale, the thermally activated nature of the embedding process may be explained by the requirement for displacement (i.e., flow) of the polymer at the vicinity of the nanoparticle while it is embedding. The displacement requires cleavage of the bonds between the polymer chains as well overcoming steric hindrances.

5 CONCLUSIONS

A novel technique was demonstrated where the glass transition of a polymer at its surface (T_{gs}) was monitored from the localized surface plasmon resonance (LSPR) of Au NPs, deposited on the polymer surface. When the temperature is increased to a critical temperature, the LSPR was found to exhibit a red shift indicative of embedding of the NPs. If we adopt this temperature as T_{gs}, then specifically for PiBMA, T_{gs} was found between 40 to 45 °C. On the other hand, the glass transition for bulk PiBMA has been reported as 55 °C. The penetration depth vs. time derived from LSPR kinetics reveal a constant speed of embedding for the NPs until the end of embedding. The speed of penetration of NPs is thermally activated and the activation energy for PiBMA was found to be 0.65 eV.

REFERENCES

[1] J. H. Teichroeb and J. A. Forrest, "Direct Imaging of Nanoparticle Embedding to Probe Viscoelasticity of Polymer Surfaces," Physical Review Letters, vol. 91, p. 016104, 2003.

[2] S. A. Hutcheson and G. B. McKenna, "Nanosphere Embedding into Polymer Surfaces: A Viscoelastic Contact Mechanics Analysis," Physical Review Letters, vol. 94, p. 076103, 2005.

[3] U. Kreibig and M. Vollmer, Optical Properties of Metal Cluster: Springer, New York, 1995.